

PAPER • OPEN ACCESS

## Laser modification of structure and optical properties of N-doped graphene oxide

To cite this article: Evgeniya Seliverstova *et al* 2021 *Mater. Res. Express* **8** 115601

View the [article online](#) for updates and enhancements.

### You may also like

- [Cation stoichiometry and electrical transport properties of the NdGaO<sub>3</sub>/\(0 0 1\)SrTiO<sub>3</sub> interface](#)  
A Kalabukhov, Yu A Boikov, I T Serenkov et al.
- [Interaction between in-gap states and carriers at the conductive interface between perovskite oxides](#)  
Chengjian Li, Weimin Jiang, Mingrui Liu et al.
- [Long-term corrosion protection of styrene acrylic coatings enhanced by fluorine and nitrogen co-doped graphene oxide](#)  
Haoran An, Yanan Gao, Shengyuan Wang et al.

Buketov University



The Electrochemical Society  
Advancing solid state & electrochemical science & technology

242nd ECS Meeting

Oct 9 – 13, 2022 • Atlanta, GA, US

Abstract submission deadline: **April 8, 2022**

Connect. Engage. Champion. Empower. Accelerate.

**MOVE SCIENCE FORWARD**



Submit your abstract



# Materials Research Express



## PAPER

# Laser modification of structure and optical properties of N-doped graphene oxide

### OPEN ACCESS

#### RECEIVED

11 September 2021

#### REVISED


6 October 2021

#### ACCEPTED FOR PUBLICATION

21 October 2021

#### PUBLISHED

2 November 2021

Evgeniya Seliverstova , Niyazbek Ibrayev , Evgeniya Menshova and Elmira Alikhaidarova

Institute of Molecular Nanophotonics, Buketov Karaganda University, Karaganda 100024, Kazakhstan

E-mail: [genia\\_sv@mail.ru](mailto:genia_sv@mail.ru)

**Keywords:** N-doped graphene oxide, laser ablation, dots, luminescence

Original content from this work may be used under the terms of the [Creative Commons Attribution 4.0 licence](https://creativecommons.org/licenses/by/4.0/).

Any further distribution of this work must maintain attribution to the author(s) and the title of the work, journal citation and DOI.



## Abstract

The effect of laser ablation of N-doped graphene oxide (NGO) sheets on its optical properties has been studied. It was shown that the average lateral size of NGO sheets was decreased from  $644.4 \pm 143.8$  to  $114.4 \pm 59.8$  nm after 60 min of ablation. The data of FTIR spectroscopy have shown that after ablation the intensity of the vibrations bands of N-containing groups increases. The optical density of NGO dispersions and the intensity of their emission are depended on the ablation time. The highest fluorescence intensity was recorded upon excitation at a wavelength of 350 nm. For all NGO samples after laser irradiation a noticeable increase in the fluorescence intensity was registered. The enhancement factor was equal to  $\sim 11.0$  and  $8.5$  times for 30 and 60 min, respectively. The lifetime of NGO fluorescence after ablation was increased from 1.73 ns to 3.63 ns. After ablation, the samples under study exhibit long-term luminescence with a maximum at about 450 nm. The data obtained open up possibilities to control the optical properties of N-doped graphene oxide and nanodots based on it.

## 1. Introduction

Carbon is one of the widespread chemical elements. Carbon materials that include graphite, diamonds, fullerenes, carbon nanotubes, and graphene have been well known for a long time.

Graphene and its derivatives are currently being actively investigated and used in the development of devices for optoelectronics [1, 2], photovoltaics [3], and photocatalysis [4, 5]. Graphene with surface oxygen-containing groups is called as graphene oxide. Graphene oxide and its modifications, in contrast to graphene, is a more convenient material for researchers, since it is easy to synthesize and use for practical purposes.

Research in the field of graphene application has recently led to a significant increase in publications dedicated to the synthesis and study of luminescent carbon and graphene dots. In comparison with traditional semiconductor quantum dots and organic dyes, photoluminescent carbon-based quantum dots are highly stable in aqueous solutions, possess by chemical inertness, photostability, biocompatibility and low toxicity [6, 7].

Various authors have shown that the optical properties of graphene dots are depended on both their structure and composition. For example, the band gap of graphene dots affects the position of the maximum of their luminescence on the wavelength scale [8]. This parameter can be modified by changing the oxidation of graphene, as well as by surface-edge states. In addition, it was demonstrated that during the chemical synthesis of graphene quantum dots [9], it is also possible to control the quantum yield of their luminescence by reducing carboxyl and epoxy groups on the surface of graphene oxide, which acts as centers of nonradiative recombination of electron-hole pairs. The authors of [10] demonstrated that doping of graphene dots with nitrogen atoms leads to a hypsochromic shift of the photoluminescence, while a decrease in defectiveness and the presence of functional groups leads to a bathochromic effect.

It is worth noting the works where the luminescence of graphene dots was studied both experimental methods and calculations. For example, in [11], the nature of the observed luminescence of graphene quantum dots doped with nitrogen and oxygen was investigated. On the basis of experimental data and the results of

calculations from first-principles it has been established that luminescence occurs mostly from surface states, and not due to recombination inside the core of a quantum dot. It is shown that the role of functional groups prevails over quantum confinement effect determining optical properties. In addition, in the work of [12] it was shown that a wide variety of spectral manifestations of the luminescence of graphene quantum dots is associated with the ratio of their size, composition, shape, and fractal inhomogeneity.

The synthesis of graphene dots is possible with 'bottom-up' and 'top-down' approaches [13]. The first method is based on the growth of a suitable precursor, for example, small molecules of aromatic hydrocarbons or polymers, into nano-sized graphene dots by catalysis reactions, hydrothermal or microwave synthesis, etc. The top-down approach implies the direct splitting of bulk carbon materials, such as soot or graphite, into nanoscale quantum dots, by liquid exfoliation or by electron beam lithography. Also, this approach can be implemented with laser ablation method. This excludes the use of additional reagents, which is especially important for luminescent objects, for example, carbon and graphene dots.

In present work, the structural and luminescence properties of nanodots based on nitrogen-doped graphene oxide (NGO) were studied. It is shown that the laser ablation method can be used to enhance NGO luminescence. Up to date there is not many papers have been published about synthesis of NGO dots by laser ablation method and their study. Meanwhile, this method is quite widespread for preparation of graphene dots based on graphene oxide [14–17]. For example, N-doped graphene dots in diethylenetriamine were prepared using laser ablation in [18]. Synthesized dots have a higher emissivity compared to undoped graphene dots. The authors of [19] proposed the method of carbon onions doping during their ablation in various N-containing solvents. In the work [20] nitrogen-doped graphene quantum dots (N-GQD) were obtained using pulsed laser ablation in dimethylformamide using a Nd:YAG laser (532 nm). The freshly prepared N-GQD structure was modified by solvothermal treatment. NGO dots have shown promising characteristics for their application in photocatalysis, photovoltaics and sensors [20–23]. However, in these works the long-term luminescence of prepared graphene dots was not studied. Meanwhile, this type of luminescence can find its application in photodynamic therapy, as well as in the development of material for the deposition of protective coatings [14, 24].

## 2. Materials and methods

NGO dots were obtained by laser ablation of NGO dispersion. Ammonia functionalized graphene oxide in water (NGO, 1 mg ml<sup>-1</sup>, Sigma Aldrich) was used. Prior to ablation, the samples were sonicated for 30 min and 5-fold diluted with deionized water (Aquamax 300). After that samples were centrifuged at 14 500 rpm for 60 min to precipitate large particles.

Ablation was carried out with second harmonics of Nd:YAG laser (LQ215, SolarLS) with  $\lambda_{\text{gen}} = 532$  nm,  $\tau_{\text{pulse}} = 8$  ns and  $E = 79$  mJ. The laser beam was focused by a lens into 0.1 cm diameter spot. During laser ablation, the dispersion was continuously mixed. The ablation time was equal to 30 and 60 min. The height of the ablated dispersion was equal to 0.8 cm.

The NGO particle size was estimated by dynamic light scattering using a Zetasizer Nano S90 analyzer (Malvern). The morphology of particles was investigated with using of TESCAN Mira-3 scanning electron microscope (SEM).

Optical properties was studied by FTIR spectroscopy with FSM 1201 spectrometer (Infraspec). Absorption spectra were measured on a Cary-300 spectrometer (Agilent). Fluorescence was obtained using an Eclipse spectrofluorimeter (Agilent). The fluorescence lifetimes were determined using the TCSPC system (Becker&Hickl) at an excitation wavelength of  $\lambda_{\text{exc}} = 375$  nm. The fluorescence lifetimes were determined by processing the decay kinetics using the SPCImage software (Becker&Hickl) as in [25, 26]. The long-lived luminescence was recorded with Eclipse spectrometer (Agilent). The spectrum and kinetics were recorded with a time delay of 0.3 ms in the time range up to 15 ms. Measurements of both fast and long-lived luminescence were carried out in cuvettes without degassing. The optical path length was equal to 1 cm.

The fluorescence quantum yield ( $\varphi_f$ ) was estimated by the relative method according to the method proposed in the [27]. Anthracene was chosen as the standard. Its fluorescence quantum yield was equal to 27% at  $\lambda_{\text{exc}} = 366$  nm [28]. The optical density of solutions, both anthracene and NGO, was the similar and equal to  $\sim 0.028$ .

## 3. Results and discussion

Average size of NGO sheets before the laser ablation was equal to  $644.4 \pm 143.8$  nm. After ablation, both the particle size and their scatter were decreased (figure 1).

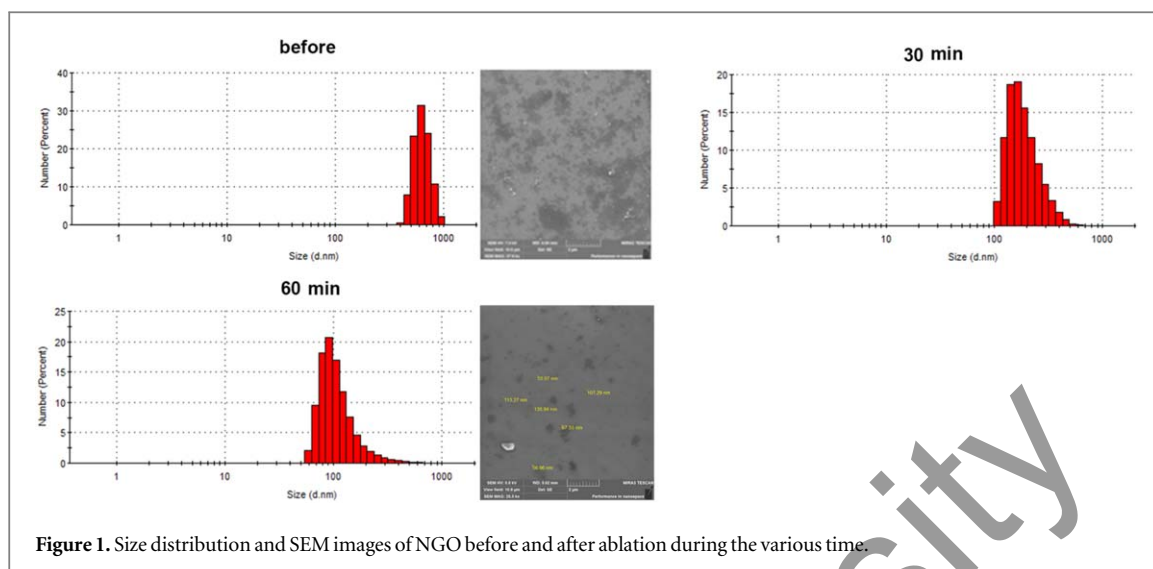


Figure 1. Size distribution and SEM images of NGO before and after ablation during the various time.

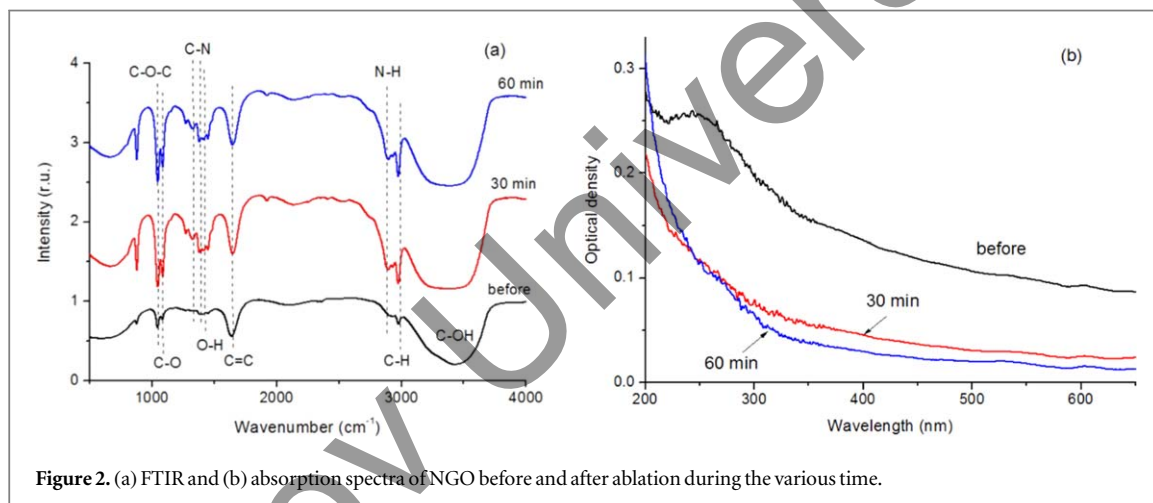


Figure 2. (a) FTIR and (b) absorption spectra of NGO before and after ablation during the various time.

The average NGO sheet diameter after 30 min ablation was equal to  $192.1 \pm 74.8$  nm. With an increase in the ablation time, a further decrease in the diameter of the NGO particles was observed. For an ablation time of 60 min, the recorded size was equal to  $114.4 \pm 59.8$  nm. SEM images of NGO before and after ablation (figure 1) showed that before ablation NGO form micrometer aggregates. After ablation, both morphology and particle size were changed markedly. As can be seen from the images obtained, wrinkles and folds are practically absent in them. Moreover, for particles obtained by ablation for 60 min, the particle sizes vary from 53 to 135 nm, which is close to the values obtained by the dynamic light scattering method. According to the definition given in [8], graphene dots are considered as sheets of graphene or its derivatives with lateral dimensions less than 100 nm.

Several bands can be distinguished in the recorded IR spectra of NGO before and after ablation (figure 2(a)). The bands around  $1058$  and  $1730$   $\text{cm}^{-1}$  are correspond to the epoxy C–O–C and carbonyl C=O stretching vibration band. The peaks at  $\sim 1090$   $\text{cm}^{-1}$  can be attributed to C–O stretching vibrations, at  $1241$  and  $3420$   $\text{cm}^{-1}$ —to C–OH stretching vibrations. A band at about  $1455$   $\text{cm}^{-1}$  can also be distinguished, which is the result of O–H deformation.

After laser treatment, the NGO spectra show an increase in the intensity of the C–N stretching vibration band; in addition, doublet bands at  $2929$  and  $2851$   $\text{cm}^{-1}$  are more pronounced, which are related to the N–H bend in the amino group [8, 20]. The band at  $\sim 1350$   $\text{cm}^{-1}$  is also more pronounced, which appears as a result of aryl C–N stretch [19]. As can be seen, some modification of the NGO structure occurs under the action of laser radiation.

Absorption spectra of NGO before and after ablation are shown in the figure 2(b). Before ablation, the absorption spectrum of NGO exhibits a maximum at 240 nm, as well as a weak shoulder at  $\sim 315$  nm. The short-wavelength band is associated with  $\pi\pi^*$ - and  $n\pi^*$ -transitions in C=C and C=O sites [29, 30]. The long-wavelength shoulder corresponds to  $\pi\pi^*$ -transitions in C=N groups [21]. After ablation, the ratio of optical

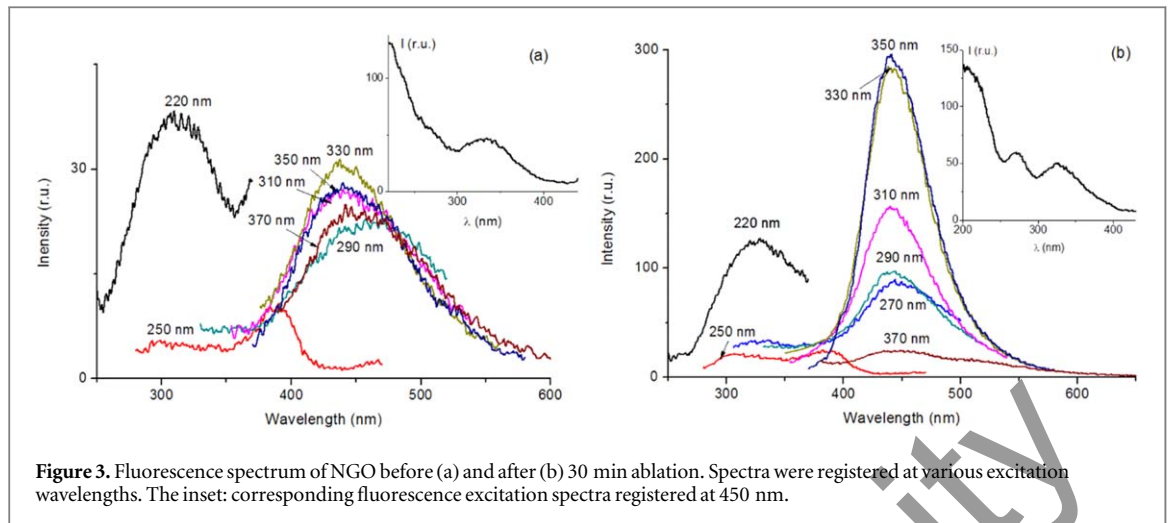


**Figure 3.** Fluorescence spectrum of NGO before (a) and after (b) 30 min ablation. Spectra were registered at various excitation wavelengths. The inset: corresponding fluorescence excitation spectra registered at 450 nm.

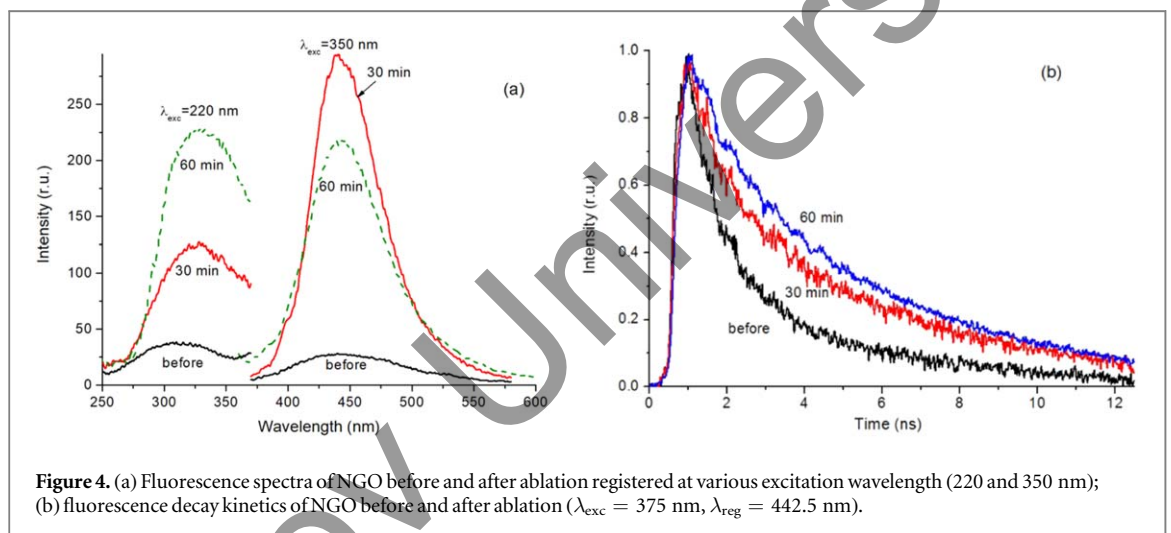


**Figure 4.** (a) Fluorescence spectra of NGO before and after ablation registered at various excitation wavelength (220 and 350 nm); (b) fluorescence decay kinetics of NGO before and after ablation ( $\lambda_{exc} = 375$  nm,  $\lambda_{reg} = 442.5$  nm).

density at 240 and 315 nm changed. At the same time, the maximal optical density is practically the same. Thus, the  $D$  value at 315 nm after ablation was decreased of 2.7 and 3.6 times for samples ablated during of 30 and 60 min, respectively.

The NGO fluorescence spectra before ablation are shown in figure 3(a). Upon photoexcitation of dispersion at 220 nm, a band exhibits with a maximum at about 305 nm. The fluorescence spectra are bathochromically shifted with an increase in excitation wavelength  $\lambda_{exc}$ . Thus, at  $\lambda_{exc} = 250$  nm along with a low-intensity band at  $\sim 300$  nm, a second luminescence band appears with a maximum at 385 nm. Subsequently it shift to the long-wavelength and exhibits at 440–450 nm. At  $\lambda_{exc} = 310$  and 370 nm the maximum fluorescence was recorded at 440 and 452 nm, respectively. It should be noted that the luminescence intensity is highest when using the  $\lambda_{exc}$  equal to 220 or 330 nm. The fluorescence excitation spectra recorded at 450 nm reveals the photoexcitation of centers absorbing in the range of 200–300 nm and 300–370 nm with a maximum at 330 nm.

Luminescence bands with the maxima at  $\sim 320$  and 440–450 nm, depending on  $\lambda_{exc}$ , were also recorded in the fluorescence spectra of NGO after ablation for 30 min (figure 3(b)). An increase in the photoexcitation wavelength leads to an intensification of the long-wavelength NGO luminescence band and a red shift of its maximum to 450 nm. The maximum intensity of NGO fluorescence was observed at  $\lambda_{exc} = 350$  nm, which coincides with the maximum of the long-wavelength band of the excitation spectrum (inset of figure 3(b)). For samples ablated for 60 min, similar position and intensity behavior of the fluorescence spectra was observed.

It should be noted that the intensity of the NGO emission after ablation is increased (figure 4(a)). Largest intensity enhancement at  $\lambda_{exc} = 220$  nm is 3.6 and 6.5 times for samples ablated for 30 and 60 min, respectively. At the same time, fluorescence was increased by  $\sim 11.0$  and 8.5 times at  $\lambda_{exc} = 350$  nm, for 30 and 60 min, respectively. The fluorescence quantum yield of NGO increased almost twofold after ablation. Its value was equal to 0.2%, 0.3% and 0.4% for samples before and after 30 and 60 min ablation, respectively. The obtained values of the  $\varphi_f$  are in agree in order of magnitude with the data published in [20].

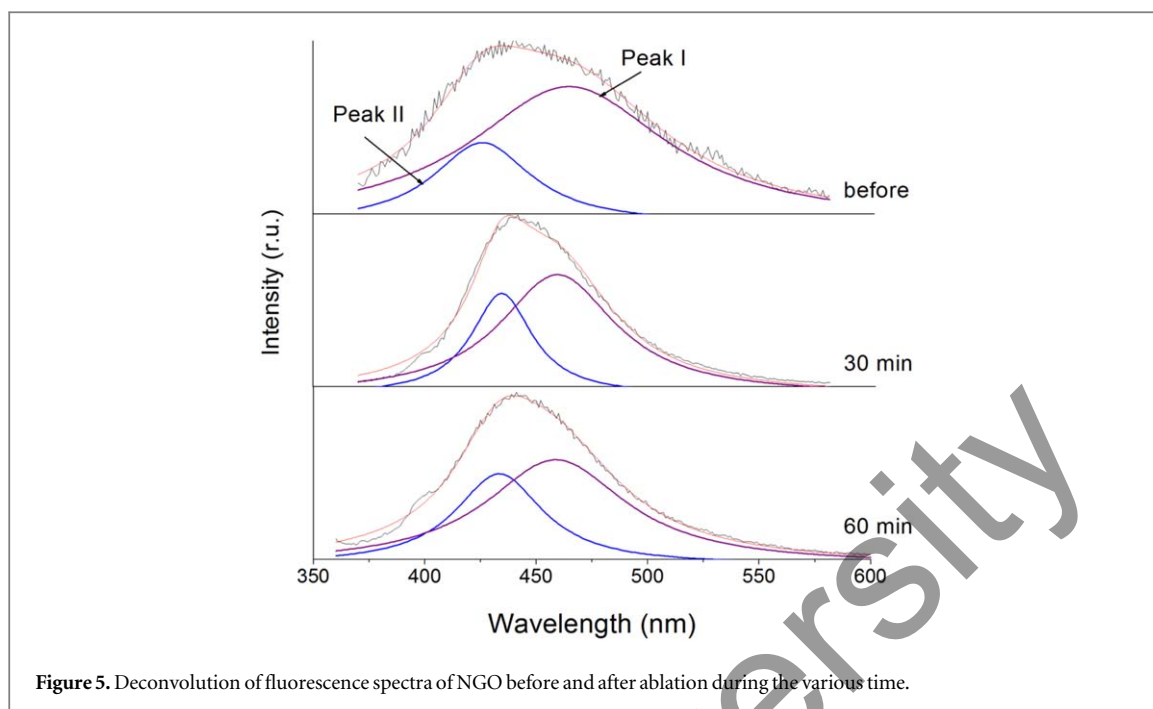


Figure 5. Deconvolution of fluorescence spectra of NGO before and after ablation during the various time.

Table 1. Fluorescence lifetime of NGO before and after ablation during the various time ( $\lambda_{\text{reg}} = 442 \text{ nm}$ ).

t (min)	$\tau_1$ (ns)	A (%)	$\tau_2$ (ns)	A (%)	$\tau_{\text{av}}$ (ns)
0	0.86	71.0	4.06	29.0	1.79
30	0.71	44.4	4.90	55.5	3.00
60	1.25	50.4	7.90	49.6	3.63

The data obtained indicate that in N-doped graphene oxide, more than one luminescence center is responsible for fluorescence. It is likely that shorter-wavelength luminescence at 300–320 nm originates from the nonuniformly distributed  $\text{sp}^2$  carbon domains. The long-wavelength fluorescence is associated with functional groups on the surface of NGO dots [18, 20]. To confirm this, the fluorescence spectra of NGO were deconvoluted by Lorentzian according to earlier works [20, 30, 31]. They report that the peak I and peak II can be assigned to  $n \rightarrow \pi^*$  and  $\pi \rightarrow \pi^*$  transitions, respectively. The first type of transition is the result of deactivation of the electronic excitation energy in functional oxygen- and nitrogen-containing groups. The second type is associated with transitions in  $\text{sp}^2$  domains in  $\text{C}=\text{C}$  in the graphene network [20]. In NGO dots before ablation (figure 5), a greater contribution to fluorescence is made by the transitions of the first type.

In ablated samples, along with peak I, the contribution from the second band also increases. This means that, along with deactivation of excitation in functional groups, radiative decay occurs in the  $\text{sp}^2$  domains of NGO. A possible mechanism could be partial reduction of oxygen groups. This is confirmed by the data of FTIR spectroscopy. In addition, fluorescence at 440 nm has been attributed by various research groups to radiation from a large proportion of hydroxyl groups.

The recorded fluorescence decay kinetics are well approximated by the biexponential law (figure 4(b), table 1). The average lifetime  $\tau_{\text{av}}$  of NGO fluorescence after ablation is increased. The main contribution to the luminescence kinetics before ablation give the fast component  $\tau_1$ , whereas after ablation, the contribution fraction is redistributed in favor of the longer luminescence component  $\tau_2$ .

Long-lived luminescence was recorded only for ablated NGO samples (figure 6) at  $\lambda_{\text{exc}} = 340 \text{ nm}$ . The luminescence was very weak under the photoexcitation at 220 nm. The maximum of the long-lived luminescence spectrum of NGO for different ablation times exhibits at 450–455 nm. The lifetime of the long-lived luminescence practically was not changed for different ablation times.

As can be seen from the data obtained, after ablation, the intensity of the long-lived luminescence of NGO increases, which may be a consequence of its structural modification. For example, it was shown in [32, 33] that phosphorescence predominates in graphene dots with a large amount of  $\text{sp}^2$  carbon due to large singlet–triplet splitting. Whereas delayed fluorescence can be recorded for the dots with a large number of oxygen-containing groups.

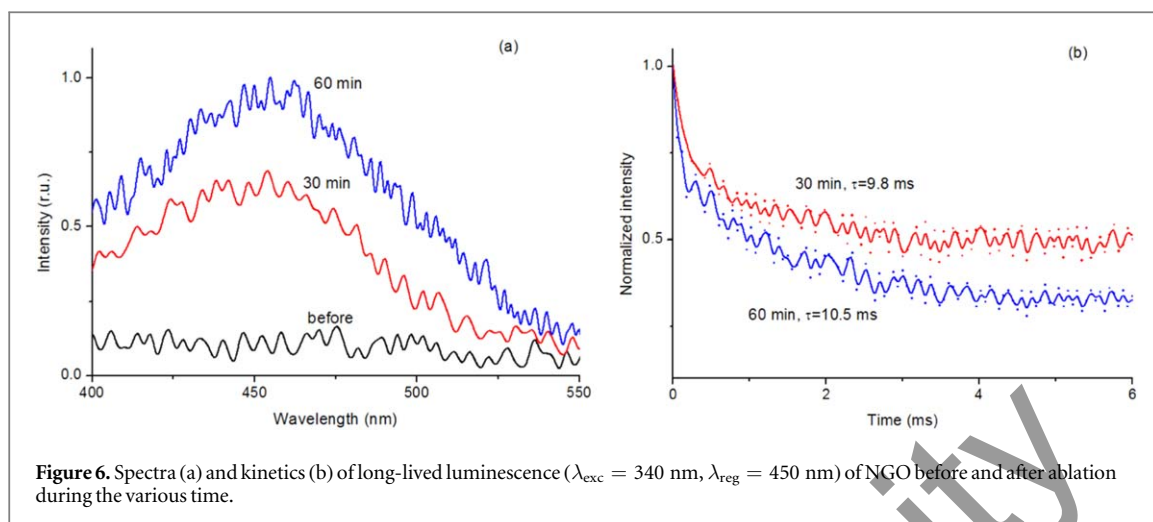


**Figure 6.** Spectra (a) and kinetics (b) of long-lived luminescence ( $\lambda_{\text{exc}} = 340$  nm,  $\lambda_{\text{reg}} = 450$  nm) of NGO before and after ablation during the various time.

## 4. Conclusion

The effect of laser ablation of nitrogen-doped graphene oxide on its optical properties was studied. It was shown that after laser ablation, the average lateral size of NGO sheets can be reduced from  $644.4 \pm 143.8$  to  $114.4 \pm 59.8$  nm. The FTIR spectra showed bands characteristic for nitrogen-doped graphene oxide. After laser irradiation, the bands associated with the vibrations of the N-containing groups were intensified. This indicates the modification of the NGO structure under the laser radiation.

It was found that the optical density at 240 and 315 nm after ablation was changed. Its value at 315 nm after ablation decreased in 2.7 and 3.6 times for 30 and 60 min, respectively. In this case, the maximum of optical density remained practically the same as before ablation.

For all samples, the intensity of fast fluorescence depends on the excitation wavelength and bathochromically shifts with its increase. The highest intensity was recorded at  $\lambda_{\text{exc}} = 350$  nm. For all samples, a noticeable increase in the fluorescence intensity by  $\sim 11.0$  and 8.5 times at  $\lambda_{\text{exc}} = 350$  nm was recorded after laser irradiation of the dispersion for 30 and 60 min, respectively. The lifetime of NGO fluorescence after ablation increases from 1.73 ns to 3.63 ns. After ablation, the samples under study exhibit long-term luminescence with a maximum at about 450 nm, which coincides with the fast fluorescence spectrum. The highest intensity of long-lived luminescence was recorded for the sample ablated for 60 min.

Thus, it has been shown that by changing the laser ablation time of the NGO one can noticeably increase its fluorescence quantum yield. The results obtained can be used for the development of organic luminescent materials, in photovoltaics, biophysics, and bioimaging.

## Acknowledgments

This work was carried out as part of the research project AP08052672, funded by the Ministry of Education and Science of the Republic of Kazakhstan.

## Data availability statement

All data that support the findings of this study are included within the article (and any supplementary files).

## Declaration of competing interest

There are no conflicts to declare.

## ORCID iDs

Evgeniya Seliverstova  <https://orcid.org/0000-0002-9507-8825>

Niyazbek Ibrayev  <https://orcid.org/0000-0002-5156-5015>

## References

- [1] Wang J G, Mu X J, Sun M T and Mu T J 2019 Optoelectronic properties and applications of graphene-based hybrid nanomaterials and van der Waals heterostructures *Appl. Mater. Today* **16** 1–20
- [2] Seliverstova E V, Ibrayev N K and Zhumabekov A Z 2020 The effect of silver nanoparticles on the photodetecting properties of the TiO<sub>2</sub>/graphene oxide nanocomposite *Opt. Spectrosc.* **128** 1449–57
- [3] Mahmoudi T, Wang Y and Hahn Y B 2018 Graphene and its derivatives for solar cells application *Nano Energy* **47** 51–65
- [4] Zhumabekov A Z, Ibrayev N K and Seliverstova E V 2020 Photoelectric properties of a nanocomposite derived from reduced graphene oxide and TiO<sub>2</sub> *Theor. Exp. Chem.* **55** 398–406
- [5] Xin L, Jiaguo Y, Wageh S, Al-Ghamdi A A and Jun X 2016 Graphene in photocatalysis: a review *Small* **12** 6640–96
- [6] Facure M H M, Schneider R, Mercante L A and Correa D S 2020 A review on graphene quantum dots and their nanocomposites: from laboratory synthesis towards agricultural and environmental applications *Environ. Sci. Nano* **7** 3710–34
- [7] Kuo W S, Yeh T S, Chang C Y, Liu J C, Chen C H, So E C and Wu P C 2020 Amino-functionalized nitrogen-doped graphene quantum dots for efficient enhancement of two-photon-excitation photodynamic therapy: functionalized nitrogen as a bactericidal and contrast agent *Int. J. Nanomedicine* **15** 6961–73
- [8] Zhu S, Song Y, Zhao X, Shao J, Zhang J and Yang B 2015 The photoluminescence mechanism in carbon dots (graphene quantum dots, carbon nanodots, and polymer dots): current state and future perspective *Nano Res.* **8** 355–81
- [9] Tetsuka H, Asahi R, Nagoya A, Okamoto K, Tajima I, Ohta R and Okamoto A 2012 Optically tunable amino-functionalized graphene quantum dots *Adv. Mater.* **24** 5333–8
- [10] Tang L, Ji R, Li X, Teng K S and Lau S P 2013 Energy-level structure of nitrogen-doped graphene quantum dots *J. Mater. Chem. C* **1** 4908–15
- [11] Dsouza S D, Buerkl M, Brunet P, Maddi C, Padmanaban D B, Morelli A, Payam A F, Maguire P, Mariotti and Svrcek V 2021 The importance of surface states in N-doped carbon quantum dots *Carbon* **183** 1
- [12] Buduka M F, Sheka E F and Popova N A 2017 Graphene quantum dots: theory and experiment *Rev. Adv. Mater. Sci.* **51** 35–49
- [13] Tian P, Tang L, Teng K S and Lau S P 2018 Graphene quantum dots from chemistry to applications *Mater. Today Chem.* **10** 221–58
- [14] Seliverstova E, Ibrayev N and Menshova E 2021 Modification of structure and optical properties of graphene oxide dots, prepared by laser ablation method *Fullerenes, Nanotubes, Carbon Nanostruct.* [Online early access]
- [15] Lin T N, Chih K H, Yuan C T, Shen J L, Lince C A J and Liud W R 2015 Laser-ablation production of graphene oxide nanostructures: from ribbons to quantum dots *Nanoscale* **7** 2708
- [16] Kang S, Kim K M, Jung K, Son Y, Mhin S, Ryu J H, Shim K B, Lee B, Han H and Song T 2019 Graphene oxide quantum dots derived from coal for bioimaging: facile and green approach *Sci. Reports* **9** 4101
- [17] Sadeghi H, Solati E and Dorrani D 2019 Producing graphene nanosheets by pulsed laser ablation: effects of liquid environment *J. Laser Appl.* **31** 042003
- [18] Santiago S R M, Lin T N, Chang C H, Wong Y A, Lin C A J, Yuan C T and Shen J L 2017 Synthesis of N-doped graphene quantum dots by pulsed laser ablation with diethylenetriamine (DETA) and their photoluminescence *Phys. Chem. Chem. Phys.* **19** 22395–400
- [19] Calabro R L, Yang D S and Kim D Y 2019 Controlled nitrogen doping of graphene quantum dots through laser ablation in aqueous solutions for photoluminescence and electrocatalytic applications *ACS Appl. Nano Mater.* **2** 6948–59
- [20] Novoa-De León I C, Johny J, Vázquez-Rodríguez S, García-Gómez N, Carranza-Bernal S, Mendivil I, Shaji S and Sepúlveda-Guzmán S 2019 Tuning the luminescence of nitrogen-doped graphene quantum dots synthesized by pulsed laser ablation in liquid and their use as a selective photoluminescence on/off probe for ascorbic acid detection *Carbon* **150** 455–64
- [21] Hasan M T, Gonzalez-Rodriguez R, Ryan C, Pota K, Green K, Coffer J L and Naumov A V 2019 Nitrogen-doped graphene quantum dots: optical properties modification and photovoltaic applications *Nano Res.* **12** 1041–7
- [22] Tabaraki R and Nateghi A 2016 Nitrogen-doped graphene quantum dots: 'turn-off' fluorescent probe for detection of Ag ions *J. Fluoresc.* **26** 297
- [23] Huang S, Qiu H, Zhu F, Lu S and Xiao Q 2015 Graphene quantum dots as on-off fluorescent probes for chromium (VI) and ascorbic acid *Microchim. Acta* **182** 1723
- [24] Aslan M and Eskalen H 2021 A study of carbon nanodots (carbon quantum dots) synthesized from tangerine juice using one-step hydrothermal method *Fullerenes, Nanotubes, Carbon Nanostruct.* **2021** [Online early access]
- [25] Seliverstova E V, Temirbayeva D A, Ibrayev N K and Ishchenko A A 2019 Plasmon effect of Ag nanoparticles on Förster resonance energy transfer in a series of cationic polymethine dyes *Theor. Exp. Chem.* **55** 115–24
- [26] Seliverstova E V, Ibrayev N K, Omarova G S, Ishchenko A A and Kucherenko M G 2021 *J. Lumin.* **235** 118000
- [27] Sahiner N, Sumer S S, Sahiner M and Silan C 2019 Nitrogen and sulfur doped carbon dots from amino acids for potential biomedical applications *J. Fluoresc.* **29** 1191
- [28] Parker C A 1968 *Photoluminescence of Solutions with Applications to Photochemistry and Analytical Chemistry* (London: Elsevier)
- [29] Gu J, Zhang Z P, Peng A M and Yang J 2016 Facile synthesis and photoluminescence characteristics of blue-emitting nitrogen-doped graphene quantum dots *Nanotechnology* **27** 165704
- [30] Li M, Cushing S K, Zhou X, Guo S and Wu N 2012 Fingerprinting photoluminescence of functional groups in graphene oxide *J. Mater. Chem.* **22** 23374
- [31] Zhang S, Li Y, Kang Y, Dong Y, Hong S and Chen X 2016 Leaky graphene oxide with high quantum yield and dual-wavelength photoluminescence *Carbon* **108** 461
- [32] Park M, Kim H S, Yoon H, Kim J, Lee S, Yoo S and Jeon S 2020 Controllable singlet-triplet energy splitting of graphene quantum dots through oxidation: from phosphorescence to TADF *Adv. Mater.* **32** 2000936
- [33] Zhu J et al 2019 Spectrally tunable solid state fluorescence and room temperature phosphorescence of carbon dots synthesized via seeded growth method *Adv. Optical Mater.* **9** 1801599